

Hypothalamic ATF3 is involved in regulating glucose and energy metabolism in mice

Y.-S. Lee · T. Sasaki · M. Kobayashi · O. Kikuchi · H.-J. Kim ·
H. Yokota-Hashimoto · M. Shimpuku · V.-Y. Susanti · Y. Ido-Kitamura ·
K. Kimura · H. Inoue · M. Tanaka-Okamoto · H. Ishizaki · J. Miyoshi ·
S. Ohya · Y. Tanaka · S. Kitajima · T. Kitamura

Received: 30 October 2012 / Accepted: 12 February 2013 / Published online: 6 March 2013
© The Author(s) 2013. This article is published with open access at Springerlink.com

Abstract

Aims/hypothesis The pancreas and hypothalamus are critical for maintaining nutrient and energy homeostasis, and combined disorders in these organs account for the onset of the metabolic syndrome. Activating transcription factor 3 (ATF3) is an adaptive response transcription factor. The physiological role of ATF3 in the pancreas has been controversial, and its role in the hypothalamus remains unknown. To elucidate the roles of ATF3 in these organs, we generated pancreas- and hypothalamus-specific *Atf3* knockout (PHT-*Atf3*-KO) mice in this study.

Methods We crossed mice bearing floxed *Atf3* alleles with *Pdx1-cre* mice, in which *cre* is specifically expressed in the pancreas and hypothalamus, and analysed metabolic

variables, pancreatic morphology, food intake, energy expenditure and sympathetic activity in adipose tissue. We also used a hypothalamic cell line to investigate the molecular mechanism by which ATF3 regulates transcription of the gene encoding agouti-related protein (*Agrp*).

Results Although PHT-*Atf3*-KO mice displayed better glucose tolerance, neither plasma glucagon nor insulin level was altered in these mice. However, these mice exhibited higher insulin sensitivity, which was accompanied by a leaner phenotype due to decreased food intake and increased energy expenditure. We also observed decreased hypothalamic *Agrp* expression in PHT-*Atf3*-KO mice. Importantly, an increase in ATF3 levels is induced by fasting or low glucose in the hypothalamus. We also showed that ATF3 interacts with forkhead box-containing protein, O subfamily 1 (FoxO1) on the *Agrp* promoter and activates *Agrp* transcription.

Conclusions/interpretation Our results suggest that ATF3 plays an important role in the control of glucose and energy metabolism by regulating *Agrp*.

Electronic supplementary material The online version of this article (doi:10.1007/s00125-013-2879-z) contains peer-reviewed but unedited supplementary material, which is available to authorised users.

Y.-S. Lee · T. Sasaki · M. Kobayashi · O. Kikuchi · H.-J. Kim ·
H. Yokota-Hashimoto · M. Shimpuku · V.-Y. Susanti ·
Y. Ido-Kitamura · T. Kitamura (✉)
Metabolic Signal Research Center, Institute for Molecular
and Cellular Regulation, Gunma University,
3-39-15, Showa-machi,
Maebashi, Gunma 371-8512, Japan
e-mail: kitamura@gunma-u.ac.jp

K. Kimura · H. Inoue
Department of Physiology and Metabolism, Brain/Liver Interface
Medicine Research Center, College of Medical, Pharmaceutical
and Health Sciences, Kanazawa University, Kanazawa, Japan

M. Tanaka-Okamoto · H. Ishizaki · J. Miyoshi
Department of Molecular Biology, Osaka Medical Center
for Cancer and Cardiovascular Diseases, Osaka, Japan

S. Ohya · Y. Tanaka · S. Kitajima
Department of Biochemical Genetics, Medical Research Institute,
Tokyo Medical and Dental University, Tokyo, Japan

Keywords *Agrp* · ATF3 · Energy expenditure · Food intake · FoxO1 · Hypothalamus

Abbreviations

AGRP	Agouti-related protein
ATF3	Activating transcription factor 3
BAT	Brown adipose tissue
Cy3	Cyanin 3
eWAT	Epididymal white adipose tissue
FoxO1	Forkhead box-containing protein, O subfamily 1
GTT	Glucose tolerance test
HFD	High-fat diet
IRS2	Insulin receptor substrate 2

ITT	Insulin tolerance test
iWAT	Inguinal white adipose tissue
Pdx1	Pancreatic and duodenal homeobox 1
PHT- <i>Atf3</i> -KO	Pancreas- and hypothalamus-specific <i>Atf3</i> knockout
RER	Respiratory exchange rate
siRNA	Small interfering RNA
SM	Skeletal muscle
Ucp1	Uncoupling protein 1

Introduction

Although its definition and aetiology remain controversial, the metabolic syndrome is considered to be the combination of type 2 diabetes, obesity, hyperlipidaemia and hypertension [1, 2]. Among these disorders, obesity is the most fundamental factor for diagnosis because increased fat cells and macrophages secrete inflammatory cytokines and induce insulin resistance, which is a key feature of the metabolic syndrome [3]. Obesity is caused by an imbalance between energy intake and energy consumption, which is also termed a failure of energy homeostasis. The most important organ for regulating energy homeostasis is the hypothalamus. The hypothalamus contains two distinct neurone types: one secretes agouti-related protein (AGRP), which increases food intake and reduces energy expenditure, and the other secretes proopiomelanocortin, which decreases food intake and increases energy expenditure [4, 5].

Recent genetic studies have revealed that insulin signalling in the hypothalamus is implicated in the regulation of energy homeostasis. Dysregulation of insulin receptor substrate 2 (IRS2) in the hypothalamus causes obesity and diabetes [6, 7]. FoxO1, an isoform of forkhead box-containing protein of the O subfamily, is a downstream effector of insulin signalling and mediates various metabolic functions of insulin [8]. We previously reported that hypothalamic FoxO1 regulates *Agrp* transcription and plays an important role in the regulation of food intake and energy expenditure [9, 10]. FoxO1 directly binds to the *Agrp* promoter, leading to the recruitment of coactivator CBP/P300 and activating *Agrp* transcription [9]. Mice that produced constitutively active FoxO1 specifically in the hypothalamus developed obesity and insulin resistance due to increased food intake and reduced energy expenditure [10].

Activating transcription factor 3 (ATF3) is a member of the ATF/CREB family of transcription factors. *Atf3* gene expression is induced by a variety of extracellular signals, including cytokines, chemokines, growth factors, hormones, hypoxia, DNA damage, endoplasmic reticulum stress and nutrient deprivation. Although *Atf3* has long been recognised as a stress-response gene, recent cumulative

evidence has suggested that ATF3 is involved in more general adaptive responses, such as environmental, emotional and nutritional alterations [11–13]. ATF3 is found in various cell types, and its disorders have been suggested to associate with inflammatory diseases, immune diseases and cancer [14]. We also previously reported that ATF3 is highly expressed in the vascular endothelial cells of human atherosclerotic lesions and is centrally involved in endothelial cell death, which might be associated with atherogenesis [15, 16].

To date, a number of studies have been conducted to elucidate the physiological roles of ATF3 in the pancreas. However, there are critical discrepancies in those studies, and the role of ATF3 in the pancreas is still controversial [17–21]. With respect to the role of ATF3 in the brain, it has been reported that ATF3 is expressed in cortical and hippocampal neurones and protects against neuronal cell death, which reduces brain damage after cerebral ischaemia [22]. ATF3 in the nucleus accumbens is reportedly critical for the regulation of emotional behaviour [13]. In contrast, although genome-wide profiling of fetal hypothalamic neurones has revealed that *Atf3* is highly expressed in the murine hypothalamus [23], its physiological role in the hypothalamus remains unknown. To elucidate these important points, we analysed knockout mice in which the ATF3 level was reduced in the pancreas and hypothalamus.

In the present study, we make two important suggestions. First, the physiological function of ATF3 in the pancreas appears to be less significant than previously predicted. Second, ATF3 has a novel, important function in the hypothalamus: hypothalamic ATF3 regulates glucose and energy metabolism by activating *Agrp* transcription.

Methods

DNA constructs, siRNA, and adenoviruses Flag-m*Atf3* was generated by PCR and subcloned into pcDNA3. PiGENE mU6 Puro-sh*Atf3* was purchased from iGENE (Tokyo, Japan). pGL3-*Agrp* and pCMV5-Flag-*FoxO1* have been previously described [9, 10]. The *FoxO1*-specific small interfering RNA (siRNA) sequence is 5'-ACG GAG GAT TGA ACC AGT ATA-3'. We have previously described Ad-*Atf3* [24].

Cell culture, transfection, adenovirus infection and luciferase assays Hypothalamic N-41 cells (Cosmo Bio, Tokyo, Japan) were maintained in high-glucose DMEM supplemented with 10% FBS. Transient transfection was performed using Lipofectamine 2000 (Invitrogen, Carlsbad, CA, USA) according to the manufacturer's instructions. Adenovirus infection was performed using a standard protocol at a multiplicity of infection (MOI) of 50. For luciferase assays, the cells were cotransfected with a reporter plasmid and the indicated

amount of expression vectors. The total amount of DNA was adjusted to 0.8 $\mu\text{g}/\text{well}$ with the addition of each corresponding empty vector. PRL-TK-*Luc* plasmid (0.1 μg) was used as an internal control.

RNA isolation and real-time RT-PCR Total RNAs were isolated from cells or tissues using RNAiso Plus (Takara, Shiga, Japan), and cDNAs were made using the Improm II Reverse Transcription System (Promega, Madison, WI, USA). cDNAs generated (1 μg) were subjected to real-time PCR using the LightCycler system and LightCycler 480 SYBR Green I (Roche, Indianapolis, IN, USA). The PCR conditions were 5 min at 95°C, followed by 40 cycles at 95°C for 10 s, 60°C for 10 s and 72°C for 10 s. The primer sequences are available upon request.

Western blot analyses Proteins from cell lysates or tissue extracts were separated by SDS-PAGE, transferred to nitrocellulose membranes (Pall Gelman Laboratory, Ann Arbor, MI, USA) and blotted with antibodies. Monoclonal antibodies against ATF3 were generated by immunising BALB/c mice with synthetic peptides derived from the carboxyl-terminal end of human/mouse ATF3, and hybridoma cell lines were established by fusing splenocytes with Sp2/0-Ag14 myeloma cells. Immunoreactive proteins were assessed by LAS-4000 Image analyser (Fuji Film, Tokyo, Japan) and densitometry using ImageJ software (NIH, Maryland, MD, USA).

Chromatin immunoprecipitation assays We performed chromatin immunoprecipitation assays in N-41 cells using the SimpleChIP^M Enzymatic Chromatin IP Kit (Cell Signaling, Danvers, MA, USA) according to the manufacturer's instructions. We used the following primers: 5'-CCT GAA AGC TTT GTC CTC TGA AGC-3' and 5'-GCA GAA CCT AGG GAT GGG TCA TGC-3', corresponding to -401 to -378 and -8 to +16 of the mouse *Agrp* gene.

Animals and analytical procedures Pancreas- and hypothalamus-specific *Atf3* knockout (PHT-*Atf3*-KO) mice were generated by crossing *Pdx1-cre* mice [25] with *Atf3*-flox mice [26]. Genotyping was performed by PCR. To detect the *Atf3*-deleted allele, we used the following primers; forward 5'-ACT GGG GCA AAG AAA CAT ACC-3' and reverse 5'-TAC CTC AGA TTT CCC TCA AAC-3'.

Mice were housed in individual cages in a temperature-controlled facility with a 12 h light/12 h dark cycle. All animal care and experimental procedures were approved by the Institutional Animal Care and Experimentation Committee at Gunma University. Mice were maintained on a 129/J \times C57BL/6J background, and their littermates were used as controls.

Blood glucose levels were measured using a glucometer (Sanwa Kagaku, Nagoya, Japan). Plasma glucagon and

insulin levels were measured by RIA (Millipore, Billerica, MA, USA) and ELISA (Shibayagi, Gunma, Japan), respectively. Plasma catecholamine levels were measured by ELISA (Cusabio, Hubei, China). For the glucose tolerance test (GTT), mice were subjected to an overnight fast followed by i.p. glucose injection (1.0 g/kg). For the insulin tolerance test (ITT), human insulin (Eli Lilly, Kobe, Japan) was injected (0.75 U/kg i.p.) to randomly fed mice. To test AKT phosphorylation, 24 h-fasted mice were injected (i.p.) with 5 U/kg of insulin. Fifteen minutes later, liver and skeletal muscle (SM) samples were subjected to western blot analysis using anti-phospho AKT (Ser473) or AKT antibody (Cell Signaling). Body weight was measured weekly, and food intake was measured daily in the dark (18:00–06:00 hours) or light (06:00–18:00 hours) phase using manual feeding hoppers. For adiposity measurement, CT was performed using a LaTheta LCT-200 (Hitachi-Aloka, Tokyo, Japan). Islets isolated from mice as described previously [27] were preincubated in Krebs–Ringer solution containing 2.8 mmol/l glucose for 15 min, and then exposed to 0.5, 10, and 25 mmol/l glucose for 1 h at 37°C. At the end of incubation, the supernatant fraction was assayed for glucagon or insulin.

Immunohistochemistry Fixed-frozen sections of mouse pancreas or hypothalamus were subjected to immunohistochemistry with anti-ATF3 (H-90; Santa Cruz, Delaware, CA, USA), anti-glucagon (Sigma, St Louis, MO, USA), anti-insulin (Dako, Carpinteria, CA, USA), anti-Ki67 (NovoCastra, Newcastle, UK), anti-caspase3 (Promega) or anti-AGRP antibody (Santa Cruz). We visualised immune complexes with FITC- or cyanin 3 (Cy3)-conjugated secondary antibodies. To quantify the percentage area of alpha cells or beta cells in relation to the pancreas, we measured the area of glucagon or insulin staining using BZ-9000 (Keyence, Osaka, Japan) and NIS-Elements (Nikon, Tokyo, Japan). We scored at least ten sections for each mouse, and six mice for each genotype. For uncoupling protein 1 (UCP1) staining, brown adipose tissue (BAT), inguinal white adipose tissue (iWAT) and epididymal white adipose tissue (eWAT) were dissected and the paraffin-sectioned slides were subjected to immunohistochemistry with anti-UCP1 antibody (Abcam, Cambridge, MA, USA). For c-fos staining, paraffin-sectioned hypothalamuses were immunostained with c-fos antibody (Santa Cruz).

Energy metabolism Measurements of oxygen consumption and carbon dioxide production were performed individually on 8-month-old mice using an Oxymax apparatus (Columbus Instruments, Columbus, OH, USA) with free access to food and water. Total oxygen consumption was calculated as the accumulated oxygen uptake for each

mouse. Respiratory exchange rate (RER) was calculated as $\dot{V}CO_2/\dot{V}O_2$. Heat generation was calculated as caloric value (CV) $\times \dot{V}O_2$, where $CV=3.815+1.232 \times RER$. Locomotor activity was measured using the ACTIMO-100 (BioResearch, Tokyo, Japan).

Statistical analyses Data are expressed as mean \pm SEM. Statistical significance was assessed by the Student's *t* test and/or one-way ANOVA using the Prism program.

Results

Tissue-specific ablation of ATF3 in the pancreas and hypothalamus of PHT-Atf3-KO mice To date, it has been controversial whether the physiological role of ATF3 in the pancreas is beneficial or detrimental to the regulation of glucose metabolism. Moreover, the role of ATF3 in the hypothalamus remains totally unknown. To clarify these important issues, we generated PHT-*Atf3*-KO mice by crossing mice bearing floxed *Atf3* alleles [26] with *Pdx1-cre* mice [25]. Although *Pdx1-cre* mice have been widely used to generate pancreas-specific gene knockout mice, the *cre* transgene is reportedly expressed in both the hypothalamus and the pancreas [10, 28]. Genotyping of DNA extracted from various organs showed that Cre-mediated excision occurred only in the islets and hypothalamus, and not in the other organs in PHT-*Atf3*-KO mice (Fig. 1a). To address the knockout efficiency of ATF3 at the protein level, we performed western blotting with anti-ATF3 antibody. ATF3 protein levels were reduced by 65% in the islets and by 75% in the hypothalamus of PHT-*Atf3*-KO mice compared with control mice, as quantified using densitometry (Fig. 1b, c). Immunohistochemical analyses also revealed that the ATF3 level was reduced in pancreatic alpha cells and beta cells (Fig. 2a), and ATF3 as well as AGRP levels were reduced in the hypothalamic area of PHT-*Atf3*-KO mice (Fig. 2b). The reduction of *Agrp* expression will be discussed below.

PHT-Atf3-KO mice have lower blood glucose levels and better glucose tolerance than control mice To investigate the effects of ATF3 ablation, we first examined blood glucose levels in PHT-*Atf3*-KO mice. Glucose levels after both fasting and random feeding were significantly lower in these mice than in the control mice (Fig. 3a, b). PHT-*Atf3*-KO mice have significantly better glucose tolerance than control mice at 2, 4 and 8 months of age (Fig. 3c, electronic supplementary material [ESM] Fig. 1a, b). Because previous reports have suggested that ATF3 plays an important role in pancreatic alpha cells or beta cells by regulating glucagon or insulin gene transcription [19, 20], we predicted that levels of plasma glucagon or insulin might be altered in PHT-*Atf3*-

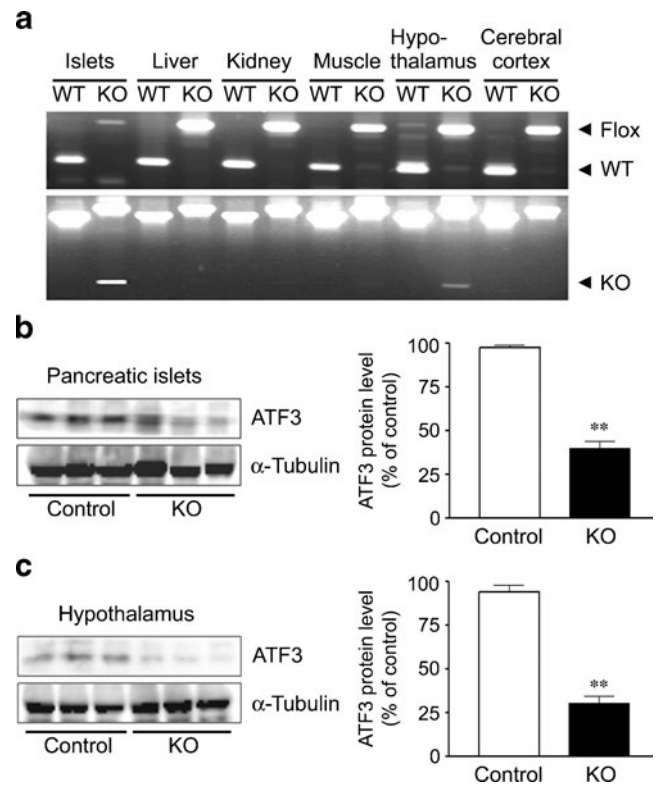
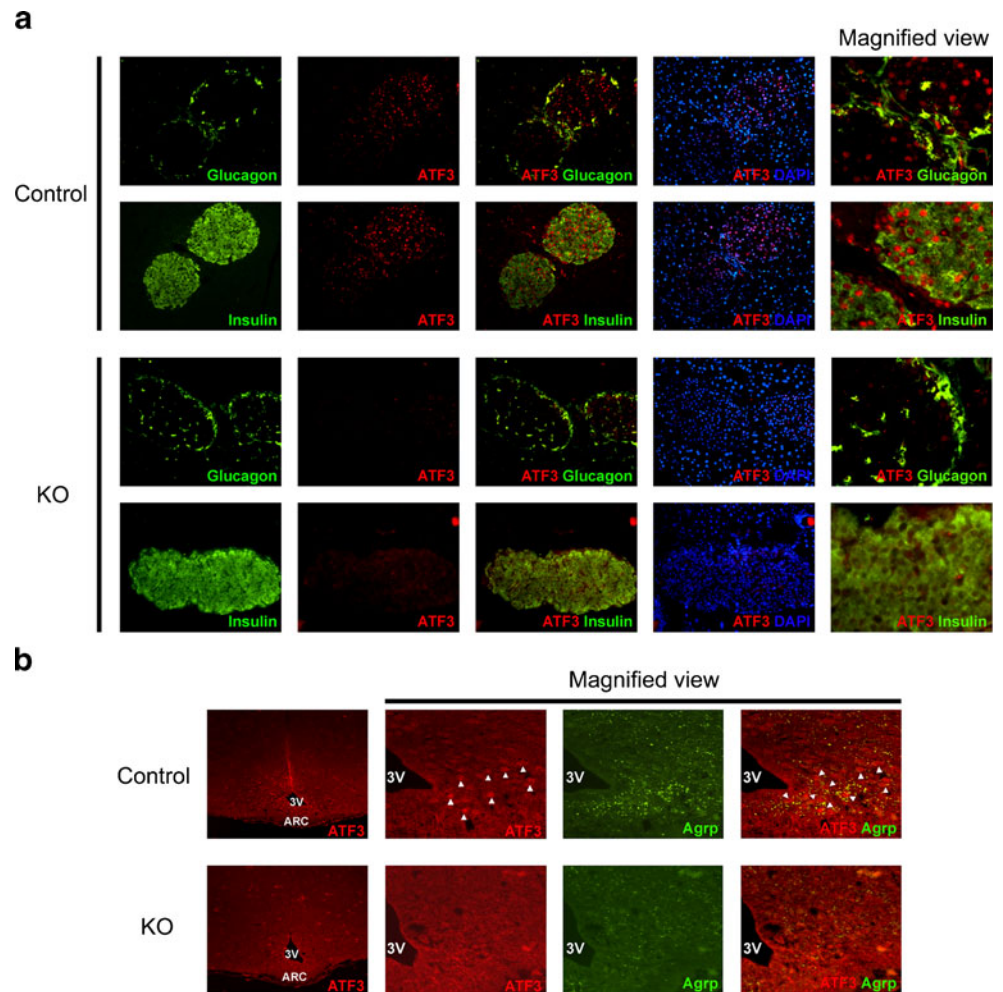


Fig. 1 Tissue-specific ablation of ATF3 in the pancreatic islets and hypothalamus of PHT-*Atf3*-KO mice. **(a)** Genotyping of DNA isolated from the pancreatic islets, liver, kidney, muscle, hypothalamus and cerebral cortex of wild-type (WT) and PHT-*Atf3*-KO (KO) mice for multiplex detection of WT and floxed alleles (top part), or for single detection of the deleted allele (bottom part). Pancreatic islets **(b)** and hypothalamus **(c)** isolated from PHT-*Atf3*-KO and control mice after 12 h of fasting were used for western blotting with anti-ATF3 monoclonal antibody. The results were normalised using α -tubulin. Densitometric analyses of the western blots are shown in the graphs on the right. Data are mean \pm SEM. ***p*<0.01

KO mice. However, plasma glucagon and insulin levels were comparable between PHT-*Atf3*-KO and control mice (Fig. 3d–g). Furthermore, plasma glucagon levels were unchanged even under severely hypoglycaemic conditions in PHT-*Atf3*-KO mice (ESM Fig. 2a).

PHT-Atf3-KO mice have normal islet function and morphology We next assessed the expression levels of glucagon and insulin 1 in islets isolated from PHT-*Atf3*-KO mice. Both the levels of *Gcg* and *Ins1* mRNAs did not differ between PHT-*Atf3*-KO and control mice (Fig. 3h, i). We also found that there was no change in the ability to secrete glucagon or insulin in response to glucose in these mice (Fig. 3j, k). Because the transgenic mice overexpressing ATF3 under the control of the *Pdx1* promoter or the *Ins1* promoter had a reduced beta cell mass [18, 21], we also assessed beta and alpha cell mass in PHT-*Atf3*-KO mice. The percentage area of alpha cells and beta cells was unchanged in PHT-*Atf3*-KO mice (ESM Fig. 2b–d).

Fig. 2 Deficiency of ATF3 expression in pancreatic alpha cells, beta cells and hypothalamus of PHT-*Atf3*-KO mice. **(a)** Frozen-sectioned pancreases from PHT-*Atf3*-KO and control mice were immunostained with anti-ATF3 (H-90) antibody, followed by Cy3-conjugated secondary antibody (red), along with anti-glucagon or anti-insulin antibody followed by FITC-conjugated secondary antibody (green) and DAPI staining (blue). $\times 200$ magnification. **(b)** After 12 h fasting, hypothalamuses were excised from PHT-*Atf3*-KO and control mice, and used for immunohistochemical analysis with anti-ATF3 (H-90) and AGRP antibody followed by Cy3 (red)- and FITC (green)-conjugated secondary antibody. $\times 100$ magnification. 3V, third ventricle; ARC, arcuate nucleus. Merged images are shown in some figure parts. Arrowheads indicate ATF3- and/or AGRP-positive neurons



Furthermore, there was no change in islet cell proliferation or apoptosis in these mice (ESM Fig. 2e, f). Taken together, these results indicate that the function and the morphology of pancreatic islets are normal in PHT-*Atf3*-KO mice.

PHT-Atf3-KO mice exhibit high insulin sensitivity and lean phenotype accompanied by reduced food intake To elucidate the reason for better glucose tolerance in PHT-*Atf3*-KO mice, despite normal islet function and morphology, we examined insulin sensitivity in these mice. The ITT revealed that PHT-*Atf3*-KO mice had significantly higher insulin sensitivity at 2, 4 and 8 months of age (Fig. 4a, ESM Fig. 3a, b). We also confirmed the higher insulin sensitivity by evaluating insulin-induced AKT phosphorylation in liver and SM, which were clearly elevated in PHT-*Atf3*-KO mice (Fig. 4b). Because PHT-*Atf3*-KO mice showed lower blood glucose levels predominantly during the later period of the ITT, we asked whether the counterregulatory response to hypoglycaemia was hampered in these mice. However, both c-fos activation in the hypothalamus and circulating catecholamine levels in response to hypoglycaemia were comparable between PHT-*Atf3*-KO and control mice, indicating

that the counterregulatory response is normal in these mice (ESM Fig. 3c, d).

Importantly, we observed that PHT-*Atf3*-KO mice were significantly leaner than control mice at all these ages (Fig. 4c). Consistent with these results, the weights of inguinal iWAT and eWAT were significantly reduced in PHT-*Atf3*-KO mice (Fig. 4d, ESM Fig. 3e). Adiposity measured by CT scanning was also decreased in PHT-*Atf3*-KO mice (Fig. 4e), while lean body mass and body length were comparable (Fig. 4f, ESM Fig. 3f). Next, we investigated the reason for the lean phenotype in PHT-*Atf3*-KO mice by measuring food intake. Daily food intake was significantly reduced in PHT-*Atf3*-KO mice compared with control mice (Fig. 4g). Furthermore, food intake in both the dark and light phases was comparably reduced in PHT-*Atf3*-KO mice (Fig. 4h, ESM Fig. 3g).

We also tested whether these mice were resistant to high-fat diet (HFD) induced metabolic disorders. Body weight was significantly lower and glucose tolerance and insulin tolerance tended to be better in PHT-*Atf3*-KO mice than in control mice under HFD conditions (Fig. 4i–k). The milder phenotype seen in HFD conditions compared with the

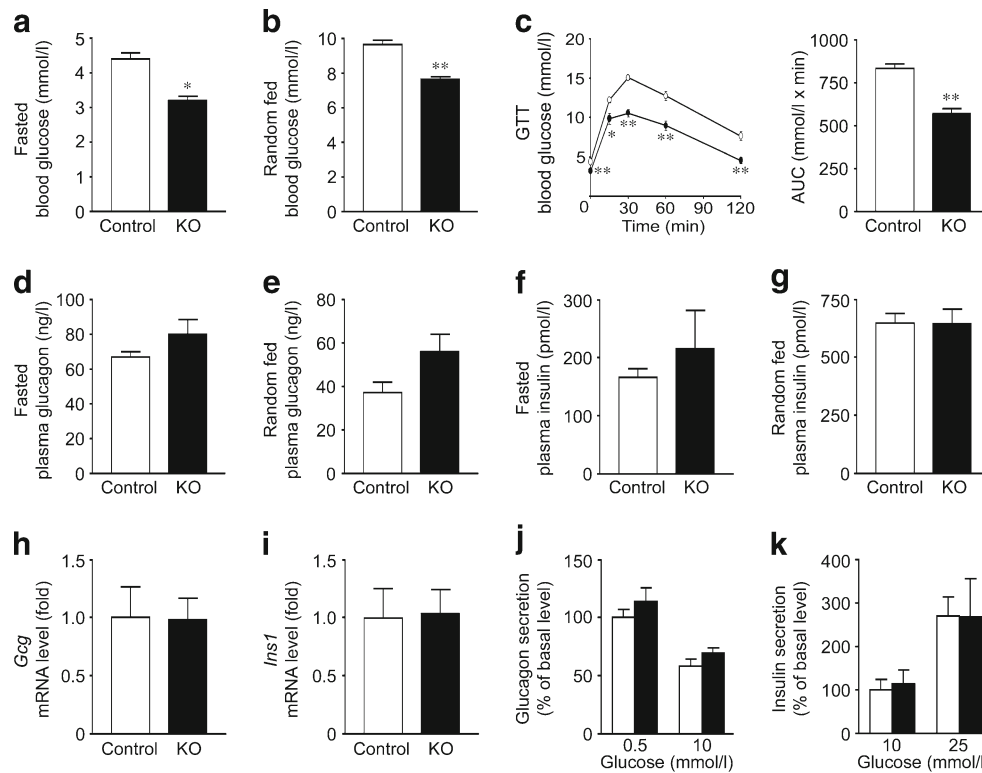


Fig. 3 Reduced blood glucose and improved glucose tolerance in PHT-*Atf3*-KO mice without alterations in plasma glucagon or insulin. Fasted (a) and randomly fed (b) blood glucose levels in PHT-*Atf3*-KO ($n=14$) and control ($n=11$) mice at 4 months of age. (c) GTTs (i.p.) in PHT-*Atf3*-KO ($n=14$) and control ($n=11$) mice at 4 months of age. White circles, control mice; black circles, PHT-*Atf3*-KO mice. AUC data for the results are also shown. Fasted and randomly fed plasma glucagon (d,e) and plasma insulin (f,g) levels in PHT-*Atf3*-KO ($n=10$)

and control ($n=10$) mice at 4 months of age. mRNA levels of *Gcg* (h) and *Ins1* (i) in the islets of PHT-*Atf3*-KO ($n=4$) and control ($n=4$) mice by real-time RT-PCR at 3 months of age. Glucagon (j) and insulin (k) secretion from the islets of PHT-*Atf3*-KO mice in response to changes in glucose concentration. The results are presented as the percentage of basal glucagon or insulin release in the control mice. Data are mean \pm SEM. * $p<0.05$, ** $p<0.01$

regular diet suggested that HFD may have attenuated the beneficial effects of ATF3 deficiency.

PHT-Atf3-KO mice have increased energy expenditure due to higher sympathetic tone and WAT to BAT conversion As another reason for the lean phenotype, we observed that oxygen consumption was significantly increased in PHT-*Atf3*-KO mice during both the light and dark phases (Fig. 5a). Accumulated oxygen consumption during the light or dark phase and 24 h oxygen consumption were also significantly increased (Fig. 5b). Carbon dioxide production, average RER and heat production were significantly increased in PHT-*Atf3*-KO mice (ESM Fig. 4a–c). In comparison, locomotor activities during these periods were unchanged in these mice (Fig. 5c). These results suggested that the increased energy expenditure was accounted for by increased basal metabolism rather than increased physical activity in PHT-*Atf3*-KO mice.

To elucidate the molecular mechanism by which basal metabolism was increased in PHT-*Atf3*-KO mice, we first investigated the expression levels of mitochondrial genes in BAT, eWAT and SM. *Pparg1a* in BAT and eWAT and *Ucp1*

in BAT were significantly increased in PHT-*Atf3*-KO mice (Fig. 5d, e). We then asked whether sympathetic tone was increased in these mice. As we expected, the expression levels of adrenergic receptors were increased in BAT, eWAT and SM of PHT-*Atf3*-KO mice (ESM Fig. 4d–f). Furthermore, PHT-*Atf3*-KO mice maintained a higher body temperature during cold exposure (Fig. 5f), which is consistent with the idea that PHT-*Atf3*-KO mice have higher sympathetic tone than control mice.

More strikingly, histological analyses using fat tissues revealed that UCP1-expressing adipocytes were increased after cold exposure in the iWAT but not the eWAT of PHT-*Atf3*-KO mice (Fig. 5g). We confirmed these results by quantitative RT-PCR and found that *Ucp1* levels were dramatically increased in the iWAT of PHT-*Atf3*-KO mice after cold exposure (Fig. 5h). *Prdm16*, a key regulator of subcutaneous WAT to BAT conversion [29, 30], tended to increase in PHT-*Atf3*-KO mice (Fig. 5i). These results indicated that PHT-*Atf3*-KO mice have high sympathetic activity in adipose tissues, causing a ‘browning’ of white adipose tissues, a rise in whole-body energy expenditure and subsequent weight loss.

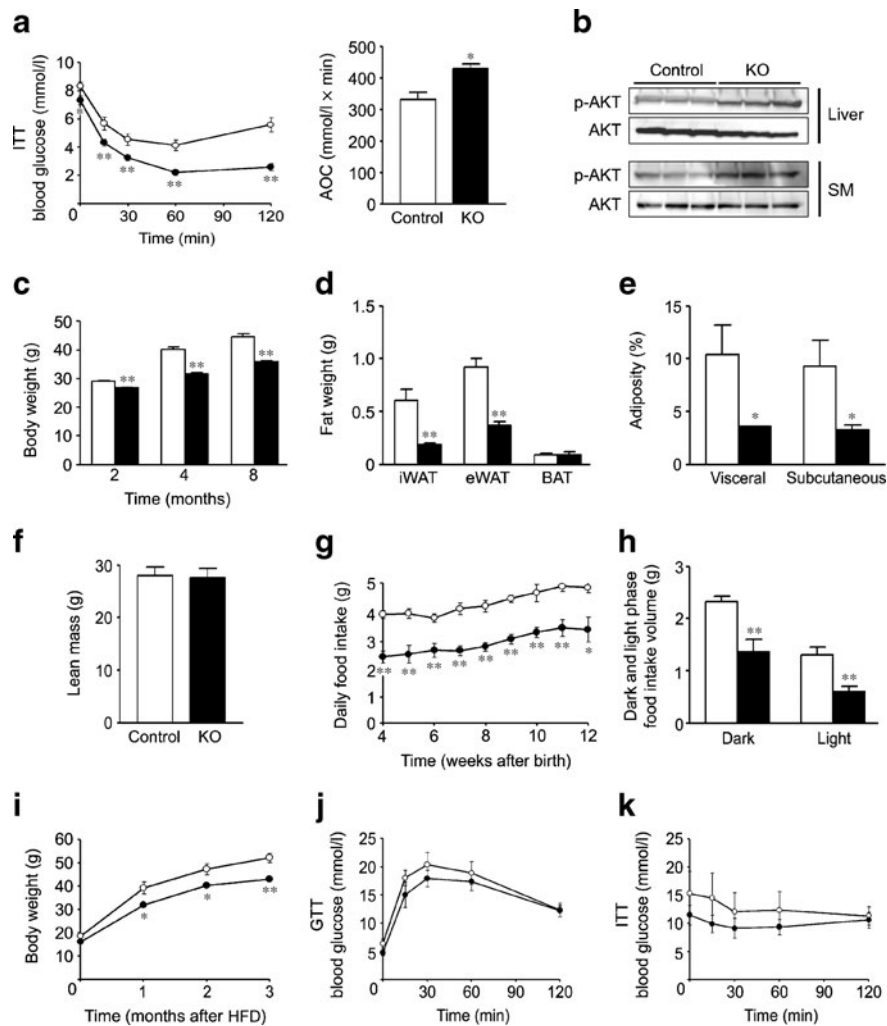


Fig. 4 Higher insulin sensitivity and lean phenotype associated with decreased food intake in PHT-*Atf3*-KO mice. **(a)** ITTs in PHT-*Atf3*-KO ($n=18$) and control ($n=12$) mice at 4 months of age. Results are shown by absolute value and decremental area over the curve (AOC). **(b)** AKT phosphorylation in liver and SM of PHT-*Atf3*-KO and control mice at 4 months ($n=3$ for each group). **(c)** Body weights of PHT-*Atf3*-KO at 2 months ($n=46$ control mice, $n=54$ KO mice), 4 months ($n=23$ control mice, $n=32$ KO mice) and 8 months ($n=19$ control mice, $n=30$ KO mice) of age. **(d)** Fat weights of PHT-*Atf3*-KO and control mice at 8 months ($n=4$ for each group). **(e)** Visceral and subcutaneous fat mass

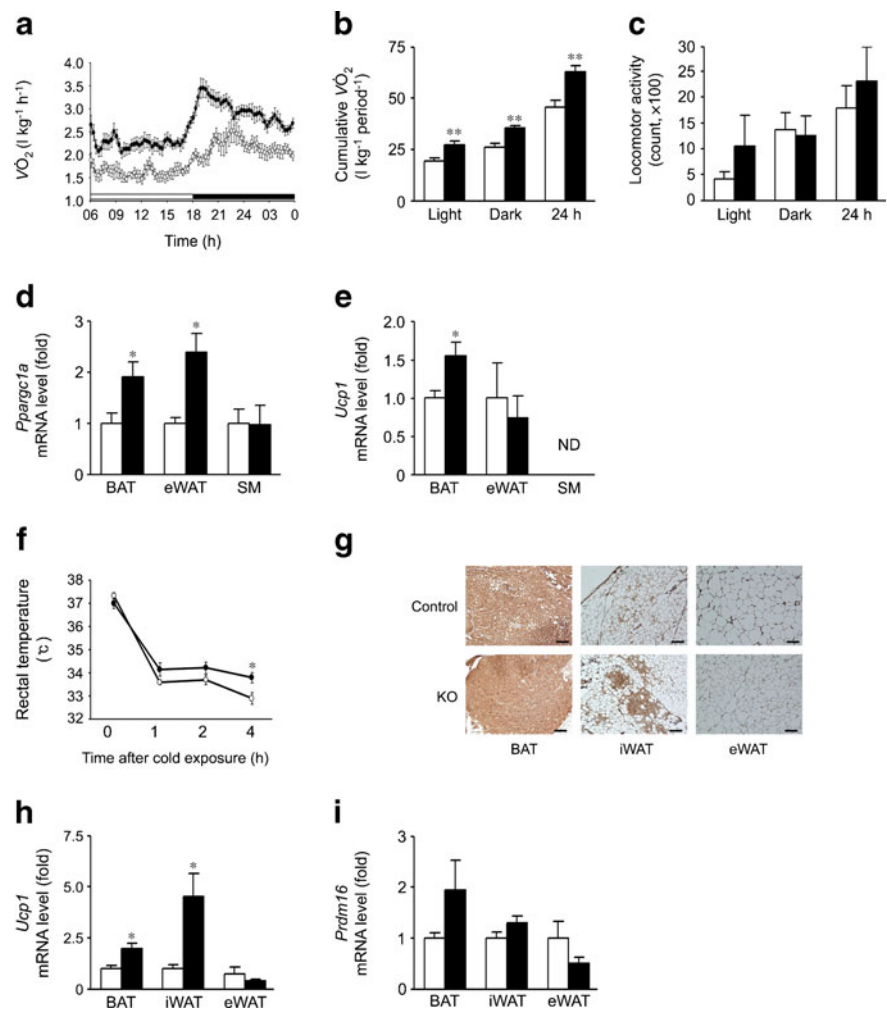
were measured in PHT-*Atf3*-KO and control mice ($n=4$ for each group). Data represent percentages of body mass. **(f)** Lean body mass of PHT-*Atf3*-KO and control mice at 3 months of age ($n=4$ for each group). **(g)** Daily food intake in PHT-*Atf3*-KO and control mice ($n=12$ for each group). **(h)** Food intake during the dark and light phases in PHT-*Atf3*-KO ($n=6$) and control ($n=7$) mice at 7 months. Body weight **(i)**, GTTs **(j)** and ITTs **(k)** in PHT-*Atf3*-KO and control mice fed an HFD starting at 4 weeks of age ($n=4$ for each group). Data are mean \pm SEM. * $p<0.05$, ** $p<0.01$

Correlative expression patterns of ATF3 and AGRP were observed in N-41 cells and mouse hypothalamus Because food intake was reduced in PHT-*Atf3*-KO mice, we assessed the expression levels of appetite-related neuropeptides in the hypothalamus and found that *Agrp* mRNA was significantly lower in PHT-*Atf3*-KO mice than in control mice (Fig. 6a), which is consistent with the reduced food intake in these mice (Fig. 4g, h). Neither *Npy*, *Pomc* nor *Hcrt* (orexin) was changed in these mice (Fig. 6a).

We then investigated the relationship between ATF3 and AGRP more precisely using the hypothalamic N-41 cell line. *Atf3* mRNA levels in N-41 cells were increased by low glucose

and reduced by high glucose, which is similar to the pattern of *Agrp* mRNA levels (Fig. 6b). Because an increase in AGRP levels is induced by fasting [9, 31], we next investigated *Atf3* mRNA levels in the hypothalamus of wild-type mice under various fasting conditions. *Atf3* mRNA levels were increased by fasting in a time-dependent manner that resembled the pattern of *Agrp* expression (Fig. 6c). We also confirmed the fasting-induced increase in ATF3 protein by western blotting (Fig. 6d). Fasting *Agrp* expression was significantly reduced in the hypothalamus of PHT-*Atf3*-KO mice compared with control mice (ESM Fig. 5a). These correlative observations suggested that ATF3 may regulate *Agrp* transcription.

Fig. 5 Increased energy expenditure due to higher sympathetic tone and conversion from WAT to BAT in PHT-*Atf3*-KO mice. Time-phased oxygen consumption (a), cumulative oxygen consumption (b) and locomotor activity (c) in PHT-*Atf3*-KO ($n=9$) and control ($n=8$) mice at 8 months of age. mRNAs levels of *Pparg1a* (d) and *Ucp1* (e) in BAT, eWAT and SM of PHT-*Atf3*-KO and control mice at 3 months of age ($n=4$ for each group); ND, not detected. (f) Rectal temperature after cold exposure at 4°C for the indicated periods ($n=4$ for each group). UCP1 immunostaining (g) and mRNA levels of *Ucp1* (h) and *Prdm16* (i) in BAT, iWAT and eWAT of PHT-*Atf3*-KO and control mice after 3 days of cold exposure at 4°C ($n=4$ for each group). White circles, control littermates; black circles, PHT-*Atf3*-KO mice. Scale bar: 10 μ M. Data are mean \pm SEM. * $p<0.05$; ** $p<0.01$. ND, no data



ATF3 regulates Agrp transcription by interacting with FoxO1 on the Agrp promoter To test whether ATF3 regulates *Agrp* transcription, we first conducted luciferase assays using the mouse *Agrp* promoter. When we cotransfected HEK293 cells or N-41 cells with *Agrp* promoter-driven luciferase vector and ATF3 expression vector, luciferase activity was increased by ATF3 expression in a dose-dependent manner, indicating that ATF3 regulates *Agrp* promoter activity (Fig. 6e).

We and others have previously reported that transcription factor FoxO1 translocates to the nucleus and becomes active in hypothalamic neurones under fasting conditions [9, 32], and that FoxO1 directly binds to the *Agrp* promoter and regulates *Agrp* transcription [9, 10]. Because the *Agrp* promoter (−401 to +16) used in the luciferase assays does not contain an ATF/CRE site but contains FoxO1 binding sites (−363 to −319 and −130 to −86), we predicted that ATF3 may regulate *Agrp* promoter activity by interacting with FoxO1. To test this hypothesis, we performed a co-immunoprecipitation assay in HEK293 cells cotransfected with ATF3 and FoxO1. HA-tagged FoxO1 co-immunoprecipitated with Flag-tagged ATF3, and conversely HA-tagged ATF3 co-

immunoprecipitated with Flag-tagged FoxO1 (Fig. 6f), indicating that ATF3 interacts with FoxO1 in intact cells. Next, we tested whether the interaction between ATF3 and FoxO1 was occurring on the *Agrp* promoter. Chromatin immunoprecipitation assay revealed that ATF3 bound to the *Agrp* promoter, including two FoxO1-binding sites, when FoxO1 was overexpressed (Fig. 6g). These results suggest that ATF3 is recruited to the *Agrp* promoter through an interaction with FoxO1.

ATF3 and FoxO1 are reciprocally required to activate Agrp transcription To investigate the roles of ATF3 and FoxO1 in the regulation of *Agrp* transcription, we measured *Agrp* promoter activity in HEK293 cells cotransfected with ATF3 and FoxO1. Coexpression of ATF3 increased FoxO1-induced *Agrp* promoter activity, while coexpression of FoxO1 increased ATF3-induced *Agrp* promoter activity in a dose-dependent manner (ESM Fig. 5b, c), indicating synergistic activation of the *Agrp* promoter by ATF3 and FoxO1.

Next, we asked whether inhibiting FoxO1 or ATF3 would affect ATF3-induced or FoxO1-induced *Agrp* promoter activity, respectively. *FoxO1* siRNA significantly reduced ATF3-

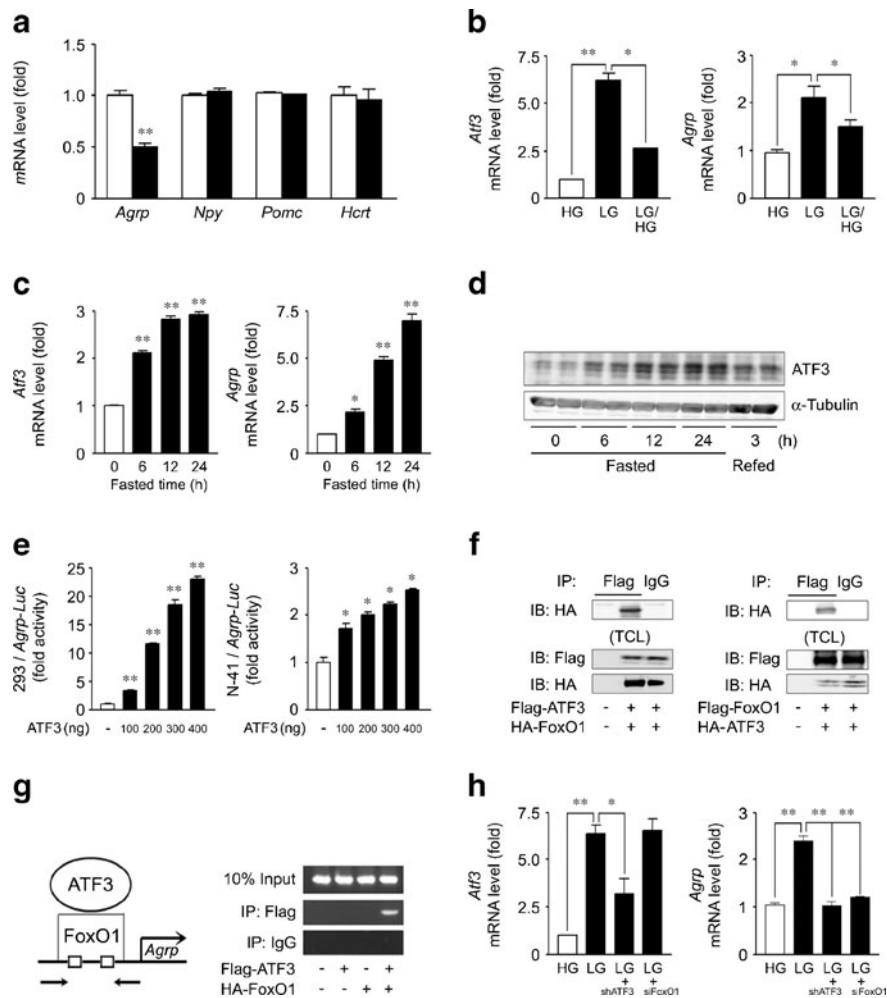


Fig. 6 ATF3 regulates *Agrp* transcription by interacting with FoxO1 on the *Agrp* promoter. **(a)** mRNA levels of *Agrp*, *Npy*, *Pomc* and *Hcrt* in the hypothalamus after 24 h of fasting at 8 months of age ($n=4$ for each group). **(b)** mRNA levels of *Atf3* and *Agrp* in N-41 cells treated with low glucose (LG) or high glucose (HG). **(c)** mRNA levels of *Atf3* and *Agrp* in the hypothalamus of wild-type mice after fasting for the periods indicated. **(d)** Hypothalamic ATF3 protein levels in wild-type mice after fasting or refeeding for the periods indicated. **(e)** *Agrp* promoter (−401 to +16)-driven luciferase (Luc) activities in HEK293 or N-41 cells transfected with ATF3 at the indicated amount of DNA.

induced *Agrp*-promoter activity in a dose-dependent manner, while *Atf3* small hairpin RNA (shRNA) partly suppressed FoxO1-induced *Agrp* promoter activity (ESM Fig. 5d, e). Furthermore, inhibition of either ATF3 or FoxO1 suppressed low glucose-induced *Agrp* expression in N-41 cells (Fig. 6h). These results demonstrated that ATF3 and FoxO1 are reciprocally required to activate *Agrp* transcription.

Discussion

Regarding double-tissue-specific knockout mice, gene ablation in one tissue may affect the phenotype resulting from

(f) Co-IP of ATF3 and FoxO1 in HEK293 cells cotransfected with ATF3 and FoxO1. HA-FoxO1 or HA-ATF3 was detected in the IP with Flag-ATF3 or Flag-FoxO1, respectively; TCL, total cell lysate. **(g)** The promoter region of the mouse *Agrp* gene. The square indicates the forkhead response element. Arrows indicate the primers used for PCR. Chromatin immunoprecipitation assays using indicated antibodies in N-41 cells cotransfected with ATF3 and FoxO1. **(h)** mRNA levels of *Atf3* and *Agrp* in N-41 cells transfected with sh*Atf3* or FoxO1 siRNA. Data are mean \pm SEM. * $p<0.05$, ** $p<0.01$. IB, immunoblot; IP, immunoprecipitation

gene ablation in another tissue. However, considering that metabolic syndrome is a combined disorder involving both the hypothalamus and the pancreas, the analyses of PHT-*Atf3*-KO mice should provide more practical insights into the relationship between ATF3 and the metabolic syndrome. Indeed, hypothalamus- and pancreas-specific IRS2 knockout mice have been used to determine the significance of combined IRS2 dysfunction in both the hypothalamus and the pancreas for the development of obesity and diabetes [6, 7].

There are several contradictions in the published literature regarding the physiological role of ATF3 in the pancreas, and the critical issue of whether pancreatic ATF3 is beneficial or detrimental to the regulation of glucose

homeostasis still remain unsolved [17]. The observations in this study—normal plasma glucagon and insulin levels (Fig. 3d–g), unchanged glucose-responsive glucagon and insulin secretion (Fig. 3j, k), and normal alpha and beta cell mass (ESM Fig. 2b–d) in PHT-*Atf3*-KO mice—suggested that the physiological role of ATF3 in the pancreas may be less significant than previously predicted, although the lower knockout efficiency of ATF3 in the pancreas (Fig. 1b) should also be considered.

Despite the unchanged islet cell morphology and function, we observed a significant decrease in blood glucose level and better glucose tolerance in PHT-*Atf3*-KO mice compared with wild-type mice (Fig. 3a–c). Therefore, we next focused on the lean phenotype and higher insulin sensitivity in these mice (Fig. 4a–e). We observed that PHT-*Atf3*-KO mice exhibited reduced food intake, which was associated with reduced *Agrp* expression in the hypothalamus (Fig. 4g, h, 6a). Although *Agrp* knockout mice were originally reported to have normal food intake, body weight and body composition [33], these mice are known to show reduced body weight and adiposity after 6 months of age [34]. Furthermore, postembryonic ablation of AGRP neurones leads to a lean phenotype due to decreased food intake and increased *Ucp1* levels in BAT [35]. We also observed that PHT-*Atf3*-KO mice have increased energy expenditure, which is associated with increased *Pparg1a* and *Ucp1* expression and increased sympathetic tone in adipose tissues (Fig. 5a–i). We further elucidated the molecular mechanism underlying these results: hypothalamic ATF3 regulates *Agrp* transcription by interacting with FoxO1. To our knowledge, all of the findings presented here regarding the role of ATF3 in the hypothalamus are novel. The limitation of this study is the lack of a pair-feeding experiment, so it is unclear to what extent the phenotype of PHT-*Atf3*-KO mice occurred secondary to reduced food intake. However, because the oxygen consumption without normalisation by body weight was still significantly increased in these mice (ESM Fig. 4g, h), higher energy expenditure was not simply due to the reduced food intake or reduced body weight. Another important finding in this study was the induction of *Atf3* expression by low glucose or fasting in a hypothalamic cell line or mouse hypothalamus (Fig. 6b–d). Because ATF3 is an adaptive response gene [14], hypothalamic ATF3 level is probably regulated by nutrient status. Additional study will be needed to clarify the mechanism that determines how changes in nutrient status regulate *Atf3* expression in the hypothalamus.

Considering that ATF3 works as a transcriptional repressor rather than an activator in most cell types [36] and that FoxO1 binds to the *Pomc* promoter and inhibits its promoter activity [9], it can be predicted that ATF3 suppresses *Pomc* gene transcription, even though the level of *Pomc* mRNA was unaltered in PHT-*Atf3*-KO mice compared with control

mice (Fig. 6a). To test this hypothesis, we performed luciferase assays using the *Pomc* promoter, including the FoxO1 binding site [9]. However, in contrast to the *Agrp* promoter, ATF3 did not affect *Pomc* promoter activity (data not shown). Therefore, hypothalamic ATF3 regulates food intake and energy expenditure by upregulating *Agrp* transcription rather than by downregulating *Pomc* transcription.

In the present study, we demonstrated that a reduction of ATF3 in the hypothalamus leads to a lean phenotype, higher insulin sensitivity and better glucose tolerance. Hypothalamic ATF3 may be a useful target for the development of a new strategy to treat or prevent obesity-based metabolic syndrome.

Acknowledgements We thank C. Osawa for excellent technical assistance and the members of the Kitamura laboratory for discussions of the data.

Funding This study was supported by Grants-in-Aid for Scientific Research (B) to T. Kitamura and the Global Centers of Excellence programme from the Ministry of Education, Culture, Sports, Science, and Technology of Japan to Y-S. Lee and T. Kitamura. This study was supported in part by the Joint Usage/Research Program of Medical Research Institute, Tokyo Medical and Dental University.

Duality of interest The authors declare that there is no duality of interest associated with this manuscript.

Contribution statement All authors contributed to the conception and design or the analysis and interpretation of data, and to drafting the article or revising it critically for intellectual content. All authors gave final approval of the version to be published.

Open Access This article is distributed under the terms of the Creative Commons Attribution Noncommercial License which permits any noncommercial use, distribution, and reproduction in any medium, provided the original author(s) and the source are credited.

References

1. Kahn R, Buse J, Ferrannini E, Stern M (2005) The metabolic syndrome: time for a critical appraisal: joint statement from the American Diabetes Association and the European Association for the Study of Diabetes. *Diabetes Care* 28:2289–2304
2. Alberti KG, Zimmet PZ (2008) Should we dump the metabolic syndrome? *BMJ* 336:641
3. Shoelson SE, Lee J, Goldfine AB (2006) Inflammation and insulin resistance. *J Clin Invest* 116:1793–1801
4. Barsh GS, Schwartz MW (2002) Genetic approaches to studying energy balance: perception and integration. *Nat Rev Genet* 3:589–600
5. Schwartz MW, Porte D Jr (2005) Diabetes, obesity, and the brain. *Science* 307:375–379
6. Kubota N, Terauchi Y, Tobe K et al (2004) Insulin receptor substrate 2 plays a crucial role in beta cells and the hypothalamus. *J Clin Invest* 114:917–927
7. Lin X, Taguchi A, Park S et al (2004) Dysregulation of insulin receptor substrate 2 in beta cells and brain causes obesity and diabetes. *J Clin Invest* 114:908–916
8. Accili D, Arden KC (2004) FoxOs at the crossroads of cellular metabolism, differentiation, and transformation. *Cell* 117:421–426

9. Kitamura T, Feng Y, Kitamura YI et al (2006) Forkhead protein FoxO1 mediates Agrp-dependent effects of leptin on food intake. *Nat Med* 12:534–540
10. Kim HJ, Kobayashi M, Sasaki T et al (2012) Overexpression of FoxO1 in the hypothalamus and pancreas causes obesity and glucose intolerance. *Endocrinology* 153:659–671
11. Montminy M (1997) Transcriptional regulation by cyclic AMP. *Annu Rev Biochem* 66:807–822
12. Hai T, Hartman MG (2001) The molecular biology and nomenclature of the activating transcription factor/cAMP responsive element binding family of transcription factors: activating transcription factor proteins and homeostasis. *Gene* 273:1–11
13. Green TA, Alibhai IN, Unterberg S et al (2008) Induction of activating transcription factors (ATFs) ATF2, ATF3, and ATF4 in the nucleus accumbens and their regulation of emotional behavior. *J Neurosci* 28:2025–2032
14. Hai T, Wolford CC, Chang YS (2010) ATF3, a hub of the cellular adaptive-response network, in the pathogenesis of diseases: is modulation of inflammation a unifying component? *Gene Expr* 15:1–11
15. Nawa T, Nawa MT, Adachi MT et al (2002) Expression of transcriptional repressor ATF3/LRF1 in human atherosclerosis: colocalization and possible involvement in cell death of vascular endothelial cells. *Atherosclerosis* 161:281–291
16. Cai Y, Zhang C, Nawa T et al (2000) Homocysteine-responsive ATF3 gene expression in human vascular endothelial cells: activation of c-Jun NH(2)-terminal kinase and promoter response element. *Blood* 96:2140–2148
17. Wang J, Webb G, Cao Y, Steiner DF (2003) Contrasting patterns of expression of transcription factors in pancreatic alpha and beta cells. *Proc Natl Acad Sci U S A* 100:12660–12665
18. Hartman MG, Lu D, Kim ML et al (2004) Role for activating transcription factor 3 in stress-induced beta-cell apoptosis. *Mol Cell Biol* 24:5721–5732
19. Wang J, Cao Y, Steiner DF (2003) Regulation of proglucagon transcription by activated transcription factor (ATF) 3 and a novel isoform, ATF3b, through the cAMP-response element/ATF site of the proglucagon gene promoter. *J Biol Chem* 278:32899–32904
20. Zmuda EJ, Qi L, Zhu MX, Mirmira RG, Montminy MR, Hai T (2010) The roles of ATF3, an adaptive-response gene, in high-fat-diet-induced diabetes and pancreatic beta-cell dysfunction. *Mol Endocrinol* 24:1423–1433
21. Li D, Yin X, Zmuda EJ et al (2008) The repression of IRS2 gene by ATF3, a stress-inducible gene, contributes to pancreatic beta-cell apoptosis. *Diabetes* 57:635–644
22. Zhang SJ, Buchthal B, Lau D et al (2011) A signaling cascade of nuclear calcium-CREB-ATF3 activated by synaptic NMDA receptors defines a gene repression module that protects against extrasynaptic NMDA receptor-induced neuronal cell death and ischemic brain damage. *J Neurosci* 31:4978–4990
23. Guerra-Crespo M, Perez-Monter C, Janga SC et al (2011) Transcriptional profiling of fetal hypothalamic TRH neurons. *BMC Genom* 12:222
24. Kawauchi J, Zhang C, Nobori K et al (2002) Transcriptional repressor activating transcription factor 3 protects human umbilical vein endothelial cells from tumor necrosis factor-alpha-induced apoptosis through down-regulation of p53 transcription. *J Biol Chem* 277:39025–39034
25. Gu G, Dubauskaite J, Melton DA (2002) Direct evidence for the pancreatic lineage: NGN3+ cells are islet progenitors and are distinct from duct progenitors. *Development* 129:2447–2457
26. Taketani K, Kawauchi J, Tanaka-Okamoto M et al (2012) Key role of ATF3 in p53-dependent DR5 induction upon DNA damage of human colon cancer cells. *Oncogene* 31:2210–2221
27. Kitamura T, Kido Y, Nef S, Merenmies J, Parada LF, Accili D (2001) Preserved pancreatic beta-cell development and function in mice lacking the insulin receptor-related receptor. *Mol Cell Biol* 21:5624–5630
28. Wicksteed B, Brissova M, Yan W et al (2010) Conditional gene targeting in mouse pancreatic ss-Cells: analysis of ectopic Cre transgene expression in the brain. *Diabetes* 59:3090–3098
29. Seale P, Conroe HM, Estall J et al (2011) Prdm16 determines the thermogenic program of subcutaneous white adipose tissue in mice. *J Clin Invest* 121:96–105
30. Ohno H, Shinoda K, Spiegelman BM, Kajimura S (2012) PPARgamma agonists induce a white-to-brown fat conversion through stabilization of PRDM16 protein. *Cell Metab* 15:395–404
31. Ebihara K, Ogawa Y, Katsuura G et al (1999) Involvement of agouti-related protein, an endogenous antagonist of hypothalamic melanocortin receptor, in leptin action. *Diabetes* 48:2028–2033
32. Fukuda M, Jones JE, Olson D et al (2008) Monitoring FoxO1 localization in chemically identified neurons. *J Neurosci* 28:13640–13648
33. Qian S, Chen H, Weingarth D et al (2002) Neither agouti-related protein nor neuropeptide Y is critically required for the regulation of energy homeostasis in mice. *Mol Cell Biol* 22:5027–5035
34. Wortley KE, Anderson KD, Yasenchak J et al (2005) Agouti-related protein-deficient mice display an age-related lean phenotype. *Cell Metab* 2:421–427
35. Bewick GA, Gardiner JV, Dhillon WS et al (2005) Post-embryonic ablation of AgRP neurons in mice leads to a lean, hypophagic phenotype. *FASEB J* 19:1680–1682
36. Chen BP, Liang G, Whelan J, Hai T (1994) ATF3 and ATF3 delta Zip. Transcriptional repression versus activation by alternatively spliced isoforms. *J Biol Chem* 269:15819–15826